Tumor-associated macrophages subvert T-cell function and correlate with reduced survival in clear cell renal cell carcinoma

Dannenmann, Stefanie Regine ; Thielicke, Julia ; Stöckli, Martina ; Matter, Claudia ; von Boehmer, Lotta ; Cecconi, Virginia ; Hermanns, Thomas ; Hefermehl, Lukas ; Schraml, Peter ; Moch, Holger ; Knuth, Alexander ; van den Broek, Maries

Abstract: Although malignant cells can be recognized and controlled by the immune system, in patients with clinically apparent cancer immunosurveillance has failed. To better understand local immunoregulatory processes that impact on cancer progression, we correlated intratumoral immunological profiles with the survival of patients affected by primary clear cell renal cell carcinoma (ccRCC). A retrospective analysis of 54 primary ccRCC samples for 31 different immune response-related transcripts, revealed a negative correlation of CD68 (a marker of tumor-associated macrophages, TAMs) and FOXP3 (a marker of regulatory T cells, Tregs) with survival. The subsequent analysis of 12 TAM-related transcripts revealed an association between the genes coding for CD163, interferon regulatory factor 4 (IRF4) and fibronectin 1 (FN1), all of which have been linked to the M2 TAM phenotype, with reduced survival and increased tumor stage, whereas the opposite was the case for the M1-associated gene coding for inducible nitric oxide synthetase (iNOS). The M2 signature of (CD68(+)) TAMs was found to correlate with CD163 expression, as determined in prospectively collected fresh ccRCC tissue samples. Upon co-culture with autologous tumor cells, CD11b(+) cells isolated from paired blood samples expressed CD163 and other M2-associated proteins, suggesting that the malignant cells promote the accumulation of M2 TAMs. Furthermore, the tumor-associated milieu as well as isolated TAMs induced the skewing of autologous, blood-derived CD4(+) T cells toward a more immunosuppressive phenotype, as shown by decreased production of effector cytokines, increased production of interleukin-10 (IL-10) and enhanced expression of the co-inhibitory molecules programmed death 1 (PD-1) and T-cell immunoglobulin mucin 3 (TIM-3). Taken together, our data suggest that ccRCC progressively attracts macrophages and induces their skewing into M2 TAMs, in turn subverting tumor-infiltrating T cells such that immunoregulatory functions are increased at the expense of effector functions.

Tumor-associated macrophages subvert T-cell function and correlate with reduced survival in clear cell renal cell carcinoma

Stefanie Regine Dannenmann,[1] Julia Thielicke,[1] Martina Stöckli,[1] Claudia Matter,[1] Lotta von Boehmer,[1] Virginia Cecconi,[1] Thomas Hermanns,[2] Lukas Hefermehl,[2] Peter Schraml,[3] Holger Moch,[3] Alexander Knuth[1] and Maries van den Broek[1,*]

[1]Department of Oncology; University Hospital Zurich; Zurich, Switzerland; [2]Department of Urology; University Hospital Zurich; Zurich, Switzerland; [3]Department of Pathology; University Hospital Zurich; Zurich, Switzerland

Although malignant cells can be recognized and controlled by the immune system, in patients with clinically apparent cancer immunosurveillance has failed. To better understand local immunoregulatory processes that impact on cancer progression, we correlated intratumoral immunological profiles with the survival of patients affected by primary clear cell renal cell carcinoma (ccRCC). A retrospective analysis of 54 primary ccRCC samples for 31 different immune response-related transcripts, revealed a negative correlation of CD68 (a marker of tumor-associated macrophages, TAMs) and FOXP3 (a marker of regulatory T cells, Tregs) with survival. The subsequent analysis of 12 TAM-related transcripts revealed an association between the genes coding for CD163, interferon regulatory factor 4 (IRF4) and fibronectin 1 (FN1), all of which have been linked to the M2 TAM phenotype, with reduced survival and increased tumor stage, whereas the opposite was the case for the M1-associated gene coding for inducible nitric oxide synthetase (iNOS). The M2 signature of (CD68+) TAMs was found to correlate with CD163 expression, as determined in prospectively collected fresh ccRCC tissue samples. Upon co-culture with autologous tumor cells, CD11b+ cells isolated from paired blood samples expressed CD163 and other M2-associated proteins, suggesting that the malignant cells promote the accumulation of M2 TAMs. Furthermore, the tumor-associated milieu as well as isolated TAMs induced the skewing of autologous, blood-derived CD4+ T cells toward a more immunosuppressive phenotype, as shown by decreased production of effector cytokines, increased production of interleukin-10 (IL-10) and enhanced expression of the co-inhibitory molecules programmed death 1 (PD-1) and T-cell immunoglobulin mucin 3 (TIM-3). Taken together, our data suggest that ccRCC progressively attracts macrophages and induces their skewing into M2 TAMs, in turn subverting tumor-infiltrating T cells such that immunoregulatory functions are increased at the expense of effector functions.

Introduction

It is well established that the immune system recognizes and can destroy tumor cells, and a significant association between immune infiltration and disease outcome has been described in many different cancers.[1] However, the interactions between immune cells and tumor cells are complex and we are only beginning to understand them. According to current models, malignant cells and immune cells mutually influence each other, ultimately resulting in the escape of the former from immunosurveillance, such as in patients with clinically manifest cancer.[2] Besides tumor cell-intrinsic escape mechanisms, including the downregulation of MHC Class I and II molecules and/or tumor-associated antigens (TAAs), neoplastic cells can create a microenvironment that interferes with immune effector mechanisms. Thus, cancer cells can secrete immunosuppressive cytokines such as interleukin (IL)-10 and transforming growth factor β (TGFβ)[3,4] and promote the recruitment of immunoregulatory cell types such as regulatory T cells (Tregs), specific subsets of tumor-associated macrophages (TAMs) and myeloid-derived suppressor cells (MDSCs).[5-7] CD68 is expressed by macrophages and preclinical data indicate that TAMs most often exert tumor-promoting functions by stimulating angiogenesis, tumor-cell proliferation and metastasis, as well as by contributing to the subversion of adaptive immune responses.[8] TAMs show a remarkable degree of plasticity and it has recently been shown that the conversion of pro-inflammatory M1 macrophages to so-called "alternatively-activated" M2 macrophages[9] and/or the preferential accumulation[10] of the

latter within neoplastic lesions exert critical tumor-promoting effects. M1 macrophages express the transcription factor interferon regulatory factor (IRF)5[11] and are thought to bear antitumor activities because of an IL-12^{high}IL-10^{low} phenotype[5] coupled to elevated expression levels of the inducible nitric oxide (NO) synthetase (iNOS),[12] resulting in increased production of NO. M2 macrophages express the transcription factor IRF4[13] and are characterized by an IL12^{low}IL10^{high} phenotype,[5] the expression of the scavenger receptor CD163,[14] the mannose receptor (MR)[15] and increased levels of fibronectin 1 (FN1).[16]

The clinical outcome of renal cell cancer (RCC) patients varies considerably, especially among individuals presenting without metastases. The prognosis for localized disease is good with a five-year survival rate of more than 90% upon tumor removal via radical or partial nephrectomy.[17] However, due to the lack of major symptoms, about one-third of patients bears metastatic disease at time of diagnosis, and 25–50% of patients treated for local disease will develop metastasis.[18] The survival of metastatic RCC is dramatically low, with a five-year survival rate of less than 15%. In this setting, treatment options are often limited by radio- and chemotherapy resistance.[19]

RCCs are largely considered as immunogenic tumors and are frequently infiltrated by immune cells.[20] However, in contrast to breast carcinoma, bladder carcinoma and other cancers (reviewed in ref. 1), an elevated number of tumor-infiltrating leukocytes (TILs) is associated with poor prognosis in RCC.[21] To better understand the local mechanisms that preclude the control of clinically apparent RCC by the immune system, we correlated intratumoral immunological profiles with survival and tumor stage (pT) in patients affected by primary clear cell renal cell carcinoma (ccRCC), which is the most frequent subtype of RCC. Furthermore, we investigated the impact of the tumor microenvironment on T-cell phenotype and function.

Results

Correlation between the expression of immune response-related transcripts and survival in ccRCC. To better understand the local immunosuppressive mechanisms that preclude the immune system to control clinically manifest RCC, we correlated intratumoral immunological profiles with survival in 54 patients affected by primary ccRCC. We retrospectively analyzed the expression of 31 immune response-related transcripts (**Table S1A**) by quantitative reverse transcription real-time PCR (qRT-PCR) using a collection of formalin-fixed paraffin-embedded (FFPE) tumor tissues from ccRCC patients, for which information on tumor size and disease course was available. The samples of patients who died of tumor-unrelated causes were excluded from the analysis (**Table S2**). Using the Cox proportional hazard model, we found no significant correlation between the degree of leukocyte infiltration (Ct values of *CD45* normalized to those of the 18S rRNA) and survival (**Fig. 1A**).

Subsequently, we quantified the transcripts of immune response-related genes upon normalization to the expression level of *CD45*, which allows for the qualitative analysis of the infiltrate independent of the degree of infiltration. We correlated each of

the 31 transcripts with survival, using Cox regression analysis (**Fig. 1A**; **Fig. S1A**). We excluded the data for lymphotoxin α (LTα), arginase 1, B and T lymphocyte associated (BTLA), IL-2 and IL-17 from the analysis because of very low or undetectable expression. Univariate Cox regression analysis revealed a significant correlation of elevated *FOXP3* (a marker of Tregs) and *CD68* (a marker of macrophages) mRNA levels with reduced survival, whereas the abundance of *CD3* transcripts (identifying T cells as a whole) did not correlate with patient survival (**Fig. 1A**). We correlated the abundance of *CD68* transcripts with that of *CD3*, *CD4* and *CD8* transcripts, finding no correlation between *CD68* and *CD3* (correlation coefficient –0.082, two-tailed p = 0.556) or *CD68* and *CD8* (correlation coefficient –0.031, two-tailed p = 0.882), but a significant correlation between *CD68* and *CD4* (correlation coefficient 0.391, two-tailed p = 0.003). The latter correlation is positive, presumably reflecting the co-existence of macrophages and regulatory T cells. Furthermore, high expression levels of perforin and tumor necrosis factor α (*TNFα*) correlated with increased survival, while high expression levels of the lymphotoxin β receptor (*LTβR*) were associated with reduced survival (**Fig. S1A**). Since these associations turned out to be significant by means of only one out of two statistical tests employed, these genes were not considered to significantly correlate with survival. No signal was observed for cytotoxic T-lymphocyte-associated protein 4 (*CTLA-4*) and *IL-10* in a few samples, and an estimated Ct value (40) was set for these samples (**Fig. S1A**). When such "no-signal" samples were excluded from the analysis, high expression values of *CTLA-4* and *IL-10* significantly correlated with reduced survival (**Fig. S1B**). Also other genes (marked with an asterisk in **Fig. S1**) failed to provide a signal in a few samples. However, statistical analyses did not significantly vary when "no-signal" samples were excluded (data not shown).

While the correlation of *FOXP3* expression levels and survival just reached the level of statistical significance using univariate Cox regression analysis, the correlation between *CD68* mRNA levels and reduced survival was independent of tumor size and patient age, as assessed by multivariate Cox regression analysis (**Fig. 1**). To validate qRT-PCR results, we quantified CD68 by immunohistochemistry on seven ccRCC tumor samples and we invariably found a clear correlation between the mRNA and protein levels of CD68 (**Fig. S2**).

The expression of M2-associated transcripts correlates with reduced survival in ccRCC. To further investigate the phenotype and impact of TAMs on ccRCC patient survival, we analyzed the same samples (**Table S2**) for the expression levels of additional 12 TAM-associated genes (**Fig 1B**; **Table S1B**; **Fig. S1C**). We found a significant correlation between decreased survival and low levels of *iNOS* or high levels of *CD163* transcripts (**Fig. 1B**). Multivariate Cox regression analysis revealed that both correlations are independent of tumor stage and patient age (**Fig. 1**). Along similar lines, a high expression of the M2-associated genes *FN1* and *IRF4* tended to correlate with reduced survival (**Fig. 1B**). Furthermore, we observed a positive correlation between the abundance of *CD163* transcripts and that of mRNAs coding for the M2-associated proteins *MR*, *IL-10* and *FN1* as well as a negative correlation between the expression levels of *CD163* and
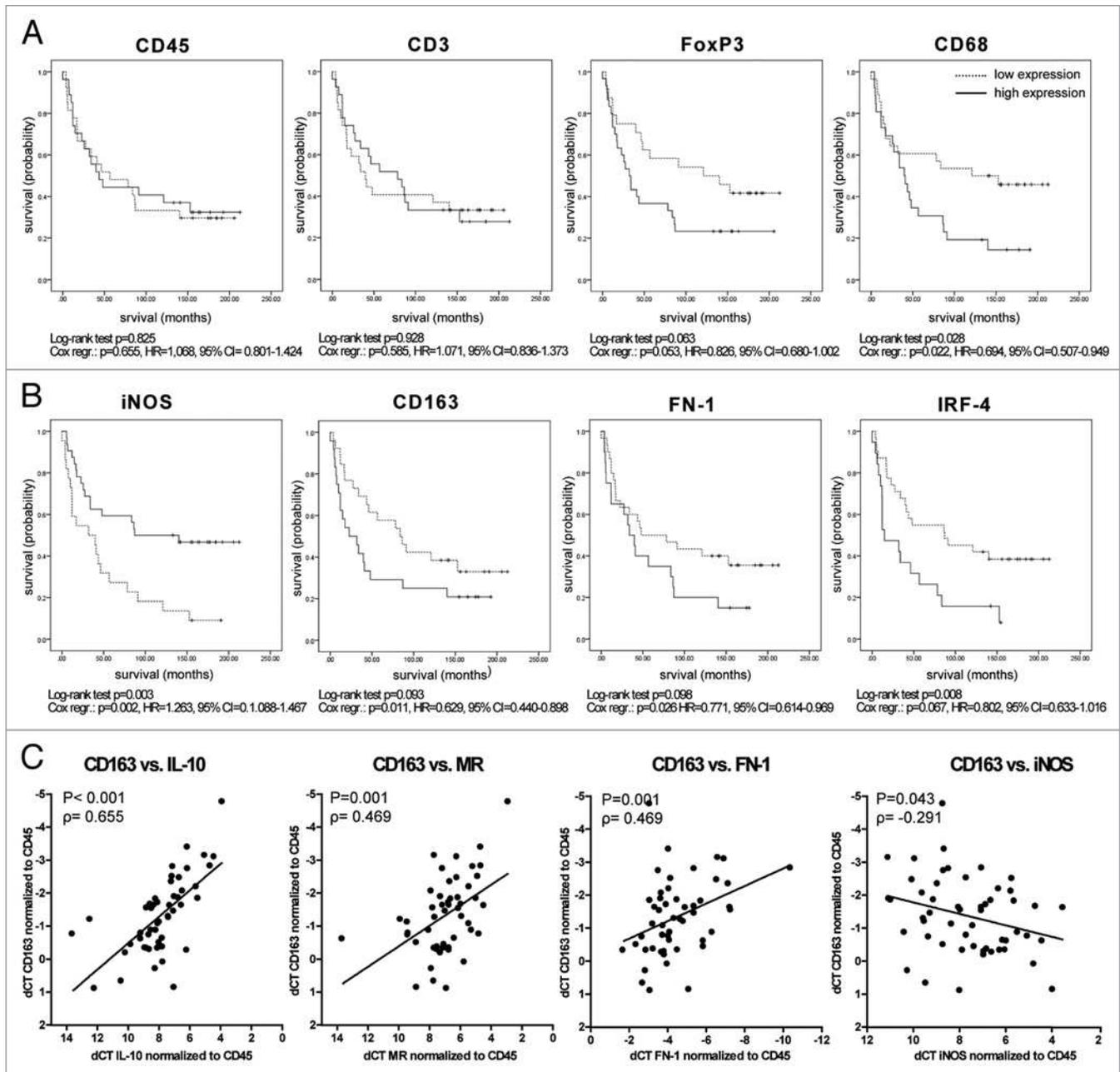
Figure 1. *FOXP3* and *CD68* and genes associated to M2 tumor-associated macrophages inversely correlate with survival in clear cell renal cell carcinoma patients. (**A–C**) Fifty-four clear cell renal cell carcinoma (ccRCC) formalin-fixed paraffin-embedded (FFPE) tumor samples were subjected to a retrospective qRT-PCR analysis for different immune response-related genes. ΔCt levels of *CD45* were calculated by normalization to the endogenous control (*18S* rRNA), ΔCt levels of all other genes were calculated by normalization to *CD45*. Survival analysis was performed using the Cox proportional hazard model and, after dichotomizing the data based on the mean-expression level, the log-rank test of the Kaplan-Meier estimator. The results of both statistical tests are displayed for selected genes. Patients that were still alive at time of analysis are marked with a tick. Kaplan-Meier survival curves show the relationship between gene expression and survival for *CD45, CD3, FOXP3 and CD68* (**A**) and *iNOS, CD163, FN1* and *IRF4* (**B**). Multivariate Cox regression analysis revealed that the correlation of target gene expression and survival is independent of tumor grade for *CD68*: p = 0.02, hazard ratio (HR) = 0.704, 95% CI 0.520–0.954; *iNOS*: p = 0.011, HR = 1.261, 95% CI 1.055–1.506 and *CD163* p = 0.015, HR = 0.645, 95% CI 0.453–0.919, as well as independent of patient age for *CD68*: p = 0.04, HR = 0.720, 95% CI 0.524–0.989; *iNOS*: p = 0.012, HR = 1.299, 95% CI 1.060–1.592 and *CD163*: p = 0.013, HR = 0.636, 95% CI 0.445–0.909. (**C**) ΔCt levels of *CD163* plotted against ΔCt values of *IL-10-, MR-, FN1-* and *iNOS*-coding transcripts. Results of Spearman Rho correlation analysis are depicted. Each dot represents an individual patient.

iNOS (an M1-associated factor) (**Fig. 1C**) suggesting that TAMs with an M2-like signature negatively influence the survival of ccRCC patients.

CD163^high TAMs exhibit an M2-phenotype. We further characterized TAMs from 12 fresh primary ccRCC tumor samples by flow cytometry. Tumors from most patients contained a

subpopulation of CD45^{+}CD3^{-}CD19^{-}CD68^{+}CD11b^{+}CD163^{high} cells (termed T_2 population hereafter), which was absent in matched peripheral blood samples. In the peripheral blood as well as in tumors, we found populations that we termed P_1 and T_1 population, respectively, both of which were characterized by a CD45^{+}CD3^{-}CD19^{-}CD68^{+}CD11b^{+}CD163^{low} phenotype (**Fig. 2A**). Both T_1 and T_2 TAMs expressed higher levels of MHC Class II molecules than P_1 cells, suggesting that TAMs exist in an activated state (**Fig. 2B**; **Fig. S4**). Based on the elevated expression of CD163 and MR, the T_2 population classifies as M2 TAMs. Furthermore, the T_2 but neither the T_1 nor the P_1 population exhibited increased expression of the programmed death ligand 1 (PD-L1) (**Fig. 2B**; **Fig. S4**). To further strengthen the presumption that CD163 associates with M2 TAMs, we analyzed the expression levels of different M1- and M2-related genes on sorted T_2 TAMs by qRT-PCR (**Table S1**). When we compared T_2 and P_1 cells for the expression of M2-associated genes, the former exhibited a strong elevation of *FN1-* and *IL-10*-coding transcripts that was accompanied by a slight increase in the expression of *IRF-4* and of the transcription factor *c-MYC*,[22] whereas the expression of the M1-associated genes *IRF5, iNOS* and *IL-12* was low (**Fig. 2C**). Except for the elevated expression of *CD163* and *MR*, no clear differences between the expression of M1- and M2-associated genes were observed in the T_2 as compared with the T_1 population, at least at the mRNA level (**Fig. S5**).

The expression of M2-associated transcripts correlates with tumor progression. RCC patients who develop metastasis have a poor prognosis, with a five-year survival rate of less than 15%.[23] We observed a similar correlation between reduced survival and the incidence of metastasis (**Fig. 3A**). High levels of *FOXP3* or *CD68* transcripts also correlated with the incidence of metastasis, whereas the expression of *CD45* and *CD3* did not (**Fig. 3B**). A correlation between tumor infiltration by macrophages and metastasis has been documented in various types of cancer.[24] In this context, a role has been proposed for the paracrine and autocrine signaling axis involving colony-stimulating factor 1 (CSF1), epidermal growth factor (EGF)[25] as well as the actin-binding protein mammalian enabled (MENA).[26] However, in our cohort of primary ccRCC patients, we did not observed a significant correlation between the expression levels of *CSF1, EGF*, their receptors and *MENA* with survival (**Fig. S1C**).

Conversely, we found a significant correlation between low *iNOS* expression levels and increased tumor stage and a similar trend for high levels of *CD163* transcripts (**Fig. 3C**). These data suggest a progressive accumulation of, or a conversion to, CD163^{high} M2 macrophages at the expense of iNOS^{high} M1 macrophages within ccRCC, which correlates with reduced patient survival.

ccRCC cells contribute to the M1 → M2 conversion of myeloid cells. To investigate whether freshly isolated ccRCC tumor cells can induce tumor-promoting changes in myeloid cells, we co-incubated P_1 cells (sorted from the peripheral blood) with autologous CD45^{-} cells (obtained from tumor samples) for 48 h at a 1:3 ratio, followed by the analysis of P_1 cells. Such a co-culture induced the upregulation of CD163 and MR in blood-derived myeloid cells, as observed at the protein level

(**Fig. S6A**). At the mRNA level, a slight increase in the expression of M2-related genes coding for *CD163, c-MYC* and *IL-10* was observed, coupled to a strong elevation in *FN1* (**Fig. S6B**). Of note, the M1-associated factor *iNOS* was upregulated in two samples, while *IL-12* was not expressed in two samples and lost in one upon co-culture with tumor cells. Because we only had sufficient material from a limited number of patients, we could not investigate this phenomenon in a larger series of samples.

In summary, the CD45^{+}CD3^{-}CD19^{-}CD68^{+}CD11b^{+}CD163^{high} T_2 population, which is found in ccRCCs but not in paired peripheral blood samples, shows features of tumor-promoting TAMs with an M2-like signature. Our findings indicating that the intratumoral levels of *CD163* transcripts correlate with reduced survival and increased tumor grade lend further support to this notion. Furthermore, we demonstrated that malignant cells favor the M1 → M2 skewing of TAMs, which is in line with the progressive accumulation of T_2 TAMs within ccRCC lesions.

The ccRCC microenvironment impacts on the phenotype and function of T cells. We noticed a correlation between high tumor stage and elevated *FOXP3* or *IL-10* expression levels (**Fig. S7**), suggesting a progressive accumulation of Tregs and IL-10 in the tumor. To investigate the impact of the immunoregulatory tumor microenvironment on the phenotype and function of T cells we sorted CD45RA^{-}CD4^{+} and CD45RA^{-}CD8^{+} T cells from fresh ccRCCs (**Table S3**) and from paired peripheral blood samples. We sorted CD45RA^{-} (antigen-experienced) T cells because the proportion of antigen-experienced T cells in tumors was much higher than in paired blood samples (**Fig. 4A**) and these T cells have a lower threshold for in vitro cytokine production upon stimulation than naïve T cells.[27] The abundance of transcripts coding for effector cytokines including *TNFα*, interferon γ (*IFNγ*), *IL-2* and for the cytotoxic molecule granzyme B was higher in tumor-derived CD4^{+} and CD8^{+} T cells than in blood-derived CD4^{+} and CD8^{+} T cells (**Fig. 4B and C**). Alongside, however, tumor-derived T cells contained elevated levels of transcripts coding for immunoregulatory molecules including programmed death 1 (*PD-1*), T-cell immunoglobulin mucin 3 (*TIM-3*) and *IL-10*. Furthermore, tumor-derived CD4^{+} T cells expressed higher levels of *FOXP3, IL-17* and the T_H2 cytokines *IL-4* and *IL-13*. Only a slight increase in TGFβ was observed in TILs, which may be explained by the fact that TGFβ is mainly regulated at a post-translational level (**Fig. 4B and C**). By flow cytometry, we confirmed that TIL-derived T cells were in an activated state, as demonstrated by the strong expression of the activation marker CD69, and confirmed the increased expression of PD-1, TIM-3, CTLA-4 and FOXP3 at the protein level (**Fig. 5A and B**; **Fig. S8**). Altogether, these data suggest that ccRCCs are sites characterized by an active immune response, which manifests features reminiscent of immune regulation or chronic inflammation.[28,29]

To confirm the alterations of the cytokine profile in tumor-derived T cells at the protein level, and to investigate the role of the tumor microenvironment on these functional deviations toward a more regulated phenotype, we polyclonally stimulated CD45RA^{-} antigen-experienced T cells in the presence of the whole tumor singe-cell suspension and compared their cytokine production profile with that of CD45RA^{-} T cells from the same
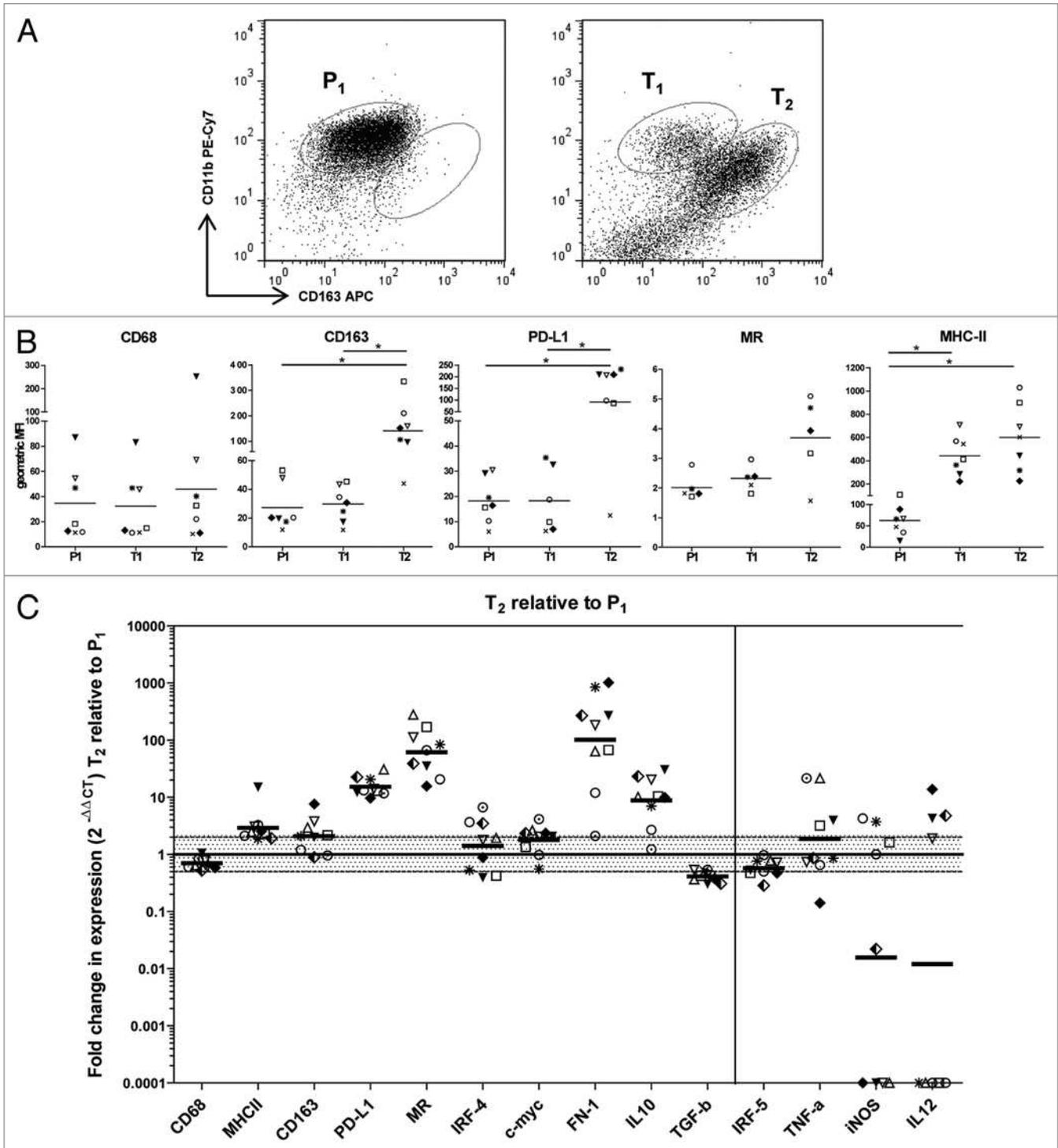
Figure 2. Characterization of tumor-associated myeloid cells in clear cell renal cell carcinoma. (**A–C**) Fresh primary clear cell renal cell carcinoma (ccRCC) and paired peripheral blood samples were collected and processed as described under *Materials and Methods*. (**A**) Dot plots display the staining of peripheral blood mononuclear cells (PBMCs, left histogram) and processed tumors (right histogram) for CD11b and CD163 after gating on $CD45^+CD3^-CD19^-$ cells. P_1, T_1 and T_2 designate individual myeloid cell populations. The plots show a representative example of one patient. (**B**) Expression of different macrophage-associated molecules after gating on P_1, T_1 and T_2 populations, displayed as the geometric mean of fluorescence intensity. Each symbol represents an individual patient; means and significant differences (*$p < 0.05$) are displayed. (**C**) qRT-PCR analysis of FACS-sorted P_1 and T_2 cell fractions. The genes displayed on the left side of the vertical line are related to M2 TAMs, on the right side to M1 TAMs. ΔCt levels were calculated upon normalization to the endogenous control *PPIA*. Results are presented as fold change in expression level of T_2 relative to P_1; the geometric mean of each group is depicted. Fold differences in expression within the shaded area are considered as not significant. Symbols at the 0.0001 line on the y-axis represent samples for which the fold change could not be calculated, since the expression was only detected the P_1 fraction. Each symbol in (**B**) and (**C**) represents an individual patient.
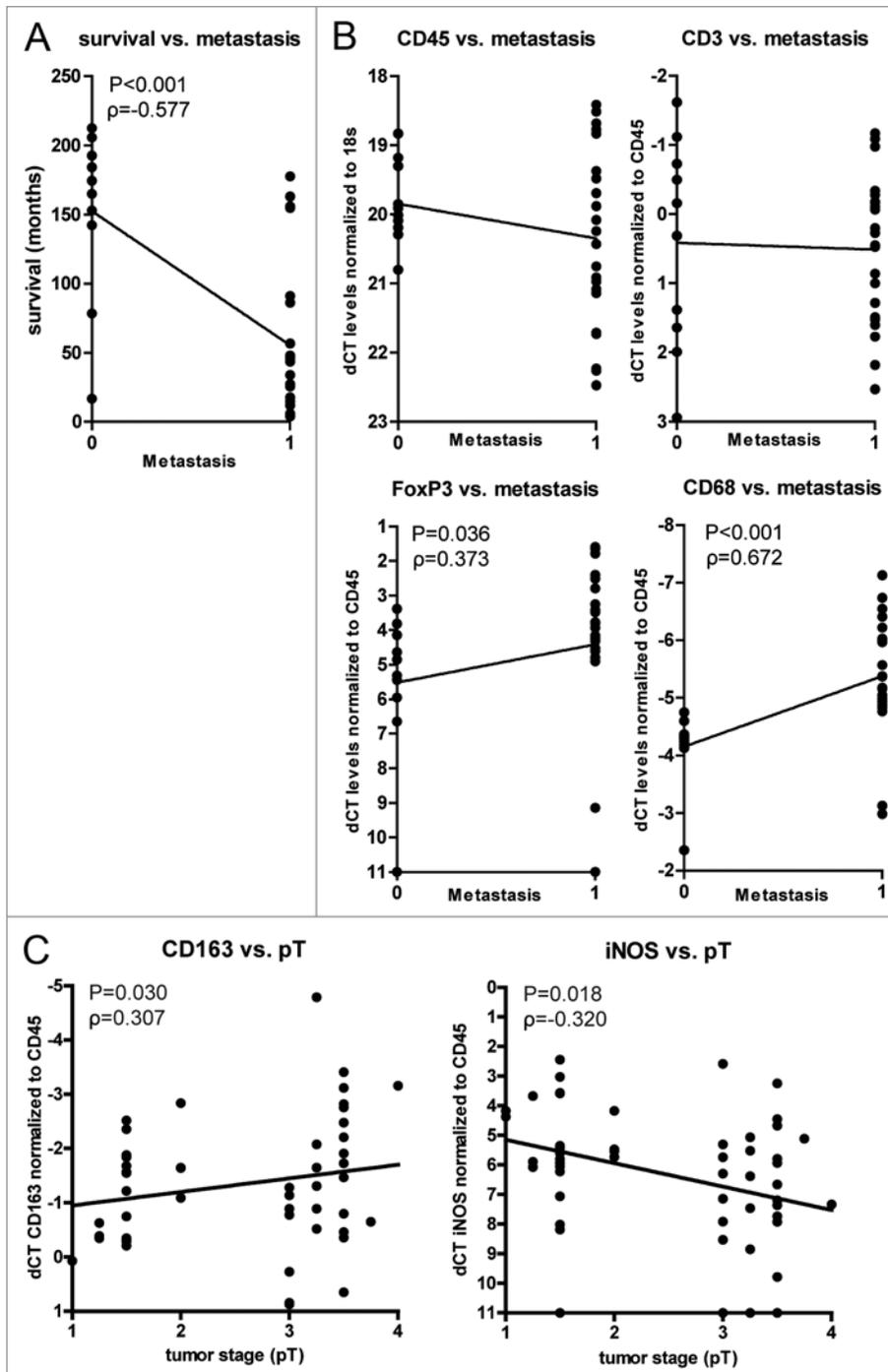
Figure 3. Positive correlation of *FOXP3* and *CD68* gene expression with the incidence of metastasis and of M2-associated genes with tumor stage. (**A**) Survival in months after diagnosis versus incidence of metastasis. (**B**) The ΔCt values of *CD45*, *CD3*, *FOXP3* and *CD68* correlated with the incidence of metastasis (0 = patient did not develop metastasis, 1 = patient developed metastasis). (**C**) The ΔCt values of *CD163* and *iNOS* correlated with tumor stage (pT). Each dot represents an individual patient. ΔCt levels were calculated as in the legend of **Figure 1**. Only when correlations are significant, the results of the Spearman Rho correlation test are displayed. Tumor stage was defined as: 1 = pT1, 1.25 = pT1a, 1.5 = pT1b, 2 = pT2, 3 = pT3, 3.25 = pT3a, 3.5 = pT3b, 3.75 = pT3c and 4 = pT4.

was lower, as compared with the same T cells in the presence of their natural tumor environment (**Fig. 6A**). The difference in effector cytokine production between sorted and non-sorted cells was less pronounced for CD8⁺ T cells, whereas the production of IL-10 was supported by the presence of the tumor (**Fig. 6B**). We detected a very low percentage of IL-17-producing cells, which was comparable in sorted and non-sorted cells (**Fig. S9**). We conclude that the tumor microenvironment induced the skewing toward a more regulated phenotype upon T-cell receptor (TCR)-dependent (anti-CD3/CD28-coated beads) as well as TCR-independent (phorbol 12-myristate 13-acetate plus ionomycin) stimulation.

M2 TAMs impact on the cytokine profile of CD4⁺ T cells. TAMs have been described to suppress tumor-specific immunity.[30,31] To investigate whether the intratumoral T₂ population contributes to the immune subversion of tumor-infiltrating antigen-experienced T cells, we stimulated sorted, blood-derived CD45RA⁻CD4⁺ cells with anti-CD3/CD28-coated beads in the presence or absence of autologous, sorted, tumor-derived T₂ (CD45⁺CD2⁻CD19⁻CD11b⁺CD163^high) cells (**Fig. S10**). Because of the limited availability of material, we could only perform TCR-dependent stimulation for CD4⁺ T cells. Peripheral blood-derived CD4⁺ T cells produced significantly less IL-2 and significantly more TGF-β, IL-10 and IL-4 upon the addition of autologous T₂ TAMs (**Fig. 7A**). The production of the effector cytokines IFNγ und TNFα followed the same trend as IL-2; although the effect was not statistically significant. Furthermore, the co-incubation with T₂ TAMs resulted in an upregulation of the transcripts coding for *PD-1* and *TIM-3* (**Fig. 7B**). No changes in T-cell function were observed when T cells were co-cultured with the sorted T₁ fraction (CD45⁺CD2⁻CD19⁻CD11b⁺CD163^low) (data not shown). There was a trend toward a reduced proliferation of T cells in the presence of the T₂ fraction, but results were not consistent (data not shown).

source that were previously sorted. The production of the effector cytokines IFNγ and IL-2 by sorted CD4⁺ T cells was higher, whereas the production of the immunoregulatory cytokine IL-10

These results indicate that CD45⁺CD2⁻CD19⁻CD11b⁺CD163^high cells contribute to functional and phenotypic immune subversion of tumor-infiltrating T cells in ccRCC patients.

Discussion

Growing evidence indicates that the immunoregulatory milieu that is associated with most tumors precludes protective antitumor immunity and compromises the efficacy of immunotherapy.[32] To better understand local immunoregulatory processes that impact on ccRCC progression, we correlated intratumoral immunological profiles with survival in patients affected by primary ccRCC. In addition, we performed functional experiments to dissect the mutual influences of tumor cells, TAMs and T cells.

We retrospectively analyzed the transcripts coding for 31 immune response-related genes in 54 FFPE primary ccRCC samples, and correlated the expression of each of these genes with survival. In line with the finding that the subtype function and location of leukocytes, rather than the degree of infiltration are relevant to disease outcome,[1] we did not observe a correlation between the extent of leukocyte *CD45* mRNA level infiltration and survival. Data on the impact of tumor infiltrating leukocytes (TILs) on ccRCC outcome are conflicting. Whereas one study has shown that an increased frequency of CD8+ T cells correlates with poor prognosis, except when these T cells are proliferating,[33] another report shows a correlation between increased T_H1 responses and improved prognosis.[34] Furthermore, it has recently been shown that an increased abundance of intratumoral lymphocytes negatively impacts the overall survival of ccRCC patients.[21] Among all lymphocyte-associated transcripts, only the expression levels of *FOXP3*, coding for a Treg-specific transcription factor[35] correlated with decreased survival, which is in line with previous findings.[36,37] Tregs are a subpopulation of T cells that play an important physiological role in suppressing effector responses to self-antigens, thereby preventing autoimmunity.[38] Furthermore, Tregs suppress antitumor immunity.[7,39] A correlation between increased numbers of intratumoral Tregs or a low ratio between effector T cells and Tregs and reduced survival has been shown in several cancer types, including ccRCC.[39,40]

We discovered that increased levels of transcripts coding for the macrophage marker CD68 correlate significantly with reduced survival in primary ccRCC patients. Although most often an increased frequency of TAMs has been correlated with unfavorable prognosis in patients affected by breast, prostate, bladder or kidney cancer, some studies involving patients bearing melanoma, gastric and colocolectal cancer report opposite findings (summarized in ref. 8). A possible explanation for these conflicting observations may be the use of the pan-macrophage marker CD68, which recognizes all the subsets of this highly heterogeneous and plastic cell population[41] and notably does not differentiate between functionally different M1 and M2 macrophages.[42,43] Pro-inflammatory M1 macrophages are induced by IFNγ and lipopolysaccharide (LPS), whereas alternatively activated, anti-inflammatory M2 macrophages differentiate in the presence of IL-4, IL-13 and IL-10.[5] M2 macrophages dampen immune and inflammatory responses to prevent tissue damage in the case of chronic inflammation.[44] Moreover, M2 macrophages promote tumor progression, metastasis and immunosuppression.[43] For this reason we expanded our retrospective analysis with 12 TAM-associated genes and found a correlation between

M1-associated factor *iNOS* and prolonged survival as well as between an increased expression of M2-associated genes (*CD163, FN1* and *IRF4*) and reduced survival. iNOS has previously been correlated with increased survival in colorectal cancer patients.[45] Furthermore, a correlation between CD163 and reduced survival has been recently observed in different types of cancer, including ccRCC.[46,47] Subsequent analysis of prospectively collected fresh tumor samples showed the presence of two different myeloid fractions in primary ccRCC lesions: CD11b+CD68+CD163high (T_2) and CD11b+CD68+CD163low (T_1) cells, whereas we only found CD11b+CD68+CD163low cells in paired peripheral blood samples (P_1 cells). The T_2 population expressed high levels of *MR, FN1* and *IL-10* and low levels of *iNOS*, thus uncovering CD163 as a marker for TAMs with an M2-like signature in ccRCC.[5,44] T_2 cells—but neither T_1 nor P_1 cells—showed increased expression of molecules that are involved in immunosuppression, including PD-L1 and IL-10. We noticed that differences in the CD163 signal between the different fractions were not as pronounced at the mRNA level as they were at the protein level. One explanation for this observation may be that *CD163* transcripts are less stable than the corresponding protein. The high level of MHC Class II molecules on the T_2 fraction clearly discriminates them from CD11b+MHC-II−/low MDSC.[6,48]

TAMs can support tumor progression in multiple ways, e.g., by promoting the survival of tumor cells, invasion, metastasis and angiogenesis.[8] Our analyses showed a correlation between *CD68* transcripts and the incidence of metastases. We observed a correlation between increased CD163 levels and tumor stage, while the opposite held true for iNOS. This suggests a progressive accumulation of M2 TAMs in ccRCC lesions, which may be due to an increased influx of M2 TAMs[10] or to the conversion of M1 to M2 macrophages in situ.[9,48,49] Our data support the second scenario, since we observed the induction of M2-associated markers on peripheral blood-derived myeloid cells upon co-culture with autologous tumor cells. These findings are in line with another study showing that the supernatants of ccRCC cell lines induce the expression of M2 markers by human macrophages.[49]

The observations that the levels of the transcripts coding for *CD163, FOXP3* and *IL-10* positively correlate with tumor stage suggests that the immune regulation increased during tumor progression.[7,50,51] Along this line, transcripts coding for the effector molecules *TNFα* and *perforin* positively correlated with survival, whereas the opposite was true for those encoding *CTLA-4* and *IL-10*. Functional TIL analysis confirmed these observations: although TILs showed an antigen-experienced (CD45RO+) and activated (CD69+, IFNγ+, TNFα+) phenotype, they simultaneously expressed high levels of PD-1, TIM-3, CTLA-4 and IL-10, all of which are indicative of ongoing immunoregulation. The increased expression of PD-1 and TIM-3 was more pronounced in tumor-derived CD8+ T cells than on their CD4+ counterparts, whereas CTLA-4 and FOXP3 expression was more prominent in tumor-derived CD4+ T cells than in CD8+ T cells. This suggests that CD4+ and CD8+ T cells may be subject to different mechanisms of immunoregulation in the tumor. In particular, the significant increase of the PD-1+/TIM-3+ population is indicative of an exhausted T-cell phenotype[52] and implies reduced effector
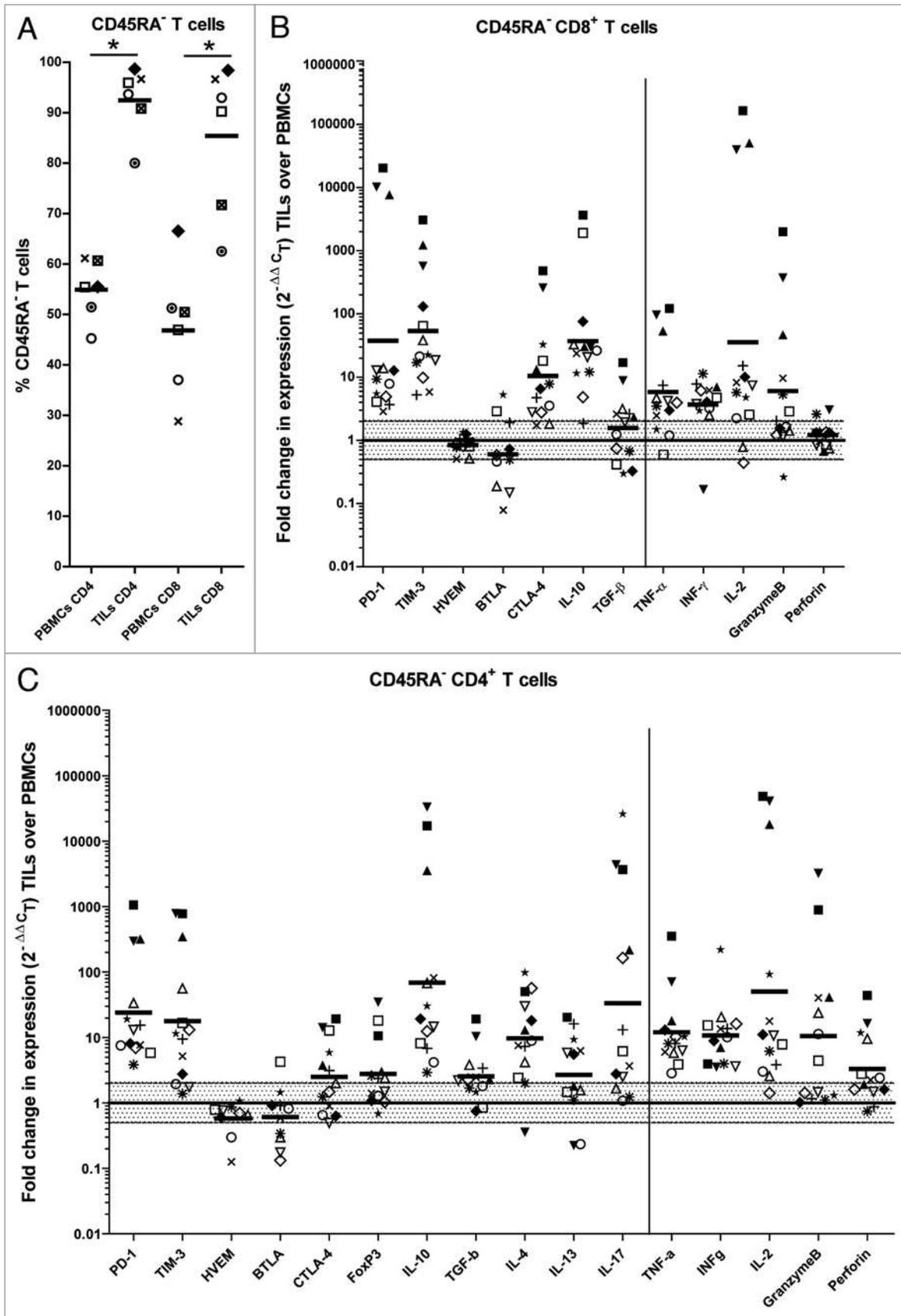
Figure 4. For figure legend, see page e23562-9.

functions of CD8⁺ T cells within ccRCCs. The tumor environment itself, or (more specifically) TAMs, contribute to the regulated phenotype of T cells because the effector functions of the latter was partially rescued by sorting CD4⁺ and CD8⁺ T cells out of the tumor. The reverse experiment, that is, the addition of sorted CD11b⁺CD163^high cells (T₂ fraction) from primary ccRCC tumor samples to autologous blood-derived CD4⁺ T cells, confirmed the negative impact of TAMs on T-cell effector function.

In conclusion, we found that an intense infiltration of primary ccRCC by Tregs and M2 TAMs correlates with reduced survival. Furthermore, we showed a progressive accumulation of (and/or the local conversion to) M2 macrophages, which is supported by tumor cells. M2 TAMs in turn induce the skewing of tumor-infiltrating T cells toward a more regulated phenotype at the expense of protective effector functions.

Materials and Methods

Paraffin embedded patient material. Formalin-fixed, paraffin-embedded material from 60 patients bearing ccRCC collected from 1993 to 2003 was identified in the archives of the Department

of Pathology, University Hospital Zurich. All patients met the following criteria: (1) a new renal tumor diagnosis with histological confirmation of a clear cell renal tumor subtype according to the 2004 WHO classification; (2) no prior treatment for renal cancer. The local ethical committee approved this study (KEK ZH, STV38-2005). Six patients died of causes not related to cancer and were excluded from the analysis. A summary of the patients' characteristics can be found in **Table S2**.

Fresh ccRCC tumor samples and blood. Twenty renal cancer patients were enrolled in the study. The patients underwent full or partial nephrectomy as part of their standard treatment at the Department of Urology, University Hospital Zurich. Tumor samples and peripheral blood were prospectively collected following informed consent in accordance with the Declaration of Helsinki. The local ethics committee and Swissmedic approved the study (EK-1017). All patients met the criteria described above. A summary of the patients' characteristics can be found in **Table S3**. Peripheral blood mononuclear cells (PBMCs) were isolated by Ficoll (Ficoll-Paque™ PLUS; GE Healthcare) density centrifugation. The tumor material was cut into multiple pieces of 2–4 mm³ and further dissociated with 6 U/mL
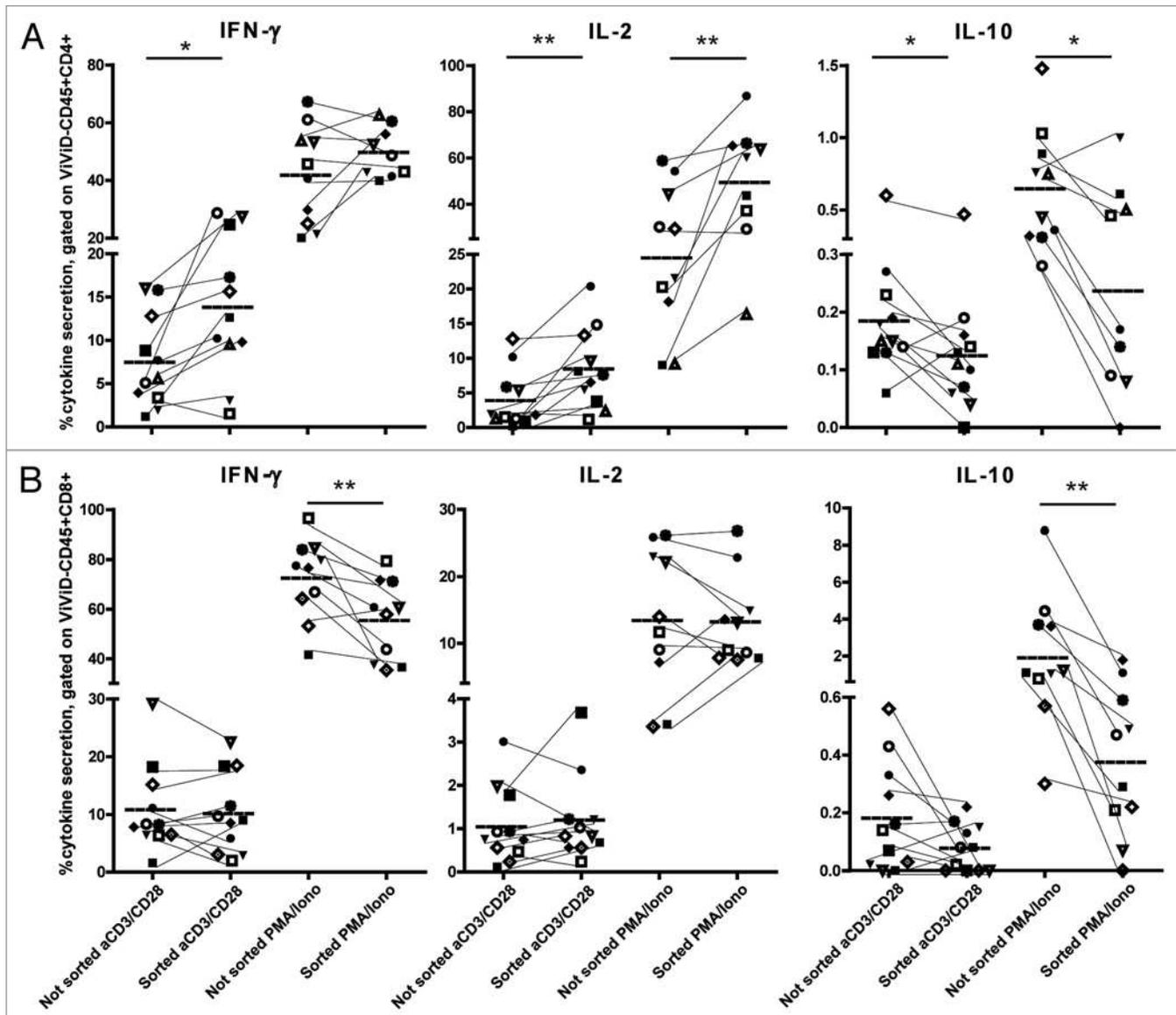
Figure 6. The tumor microenvironment impacts on the cytokine profile of T cells. Intracellular staining for cytokines after 6 h ex vivo stimulation with anti-CD3/CD28 beads or with phorbol 12-myristate 13-acetate (PMA) + ionomycin in the presence of brefeldin A and monensin. Cells were stimulated within the tumor single-cell suspension or after sorting of CD45$^+$CD4$^+$ T cells (**A**) or CD45$^+$CD8$^+$ T cells (**B**) and analyzed after gating on live CD45$^+$CD4$^+$ T cells (**A**) or live CD45$^+$CD8$^+$ T cells (**B**). Each symbol represents an individual patient. Results of unsorted and sorted T cells from the same patient are connected by a thin line. The mean of each group and significant differences (*p < 0.05; **p < 0.005) are depicted.

DNase I Type IV (Sigma) and 1 mg/mL collagenase IV (Sigma) in DMEM (Gibco) plus 50 U/mL penicillin and 50 U/mL streptomycin (Gibco) for 1–2 h at 37°C. The digested material was afterwards filtered and single-cell suspensions and the PBMCs were cryopreserved at -80°C until further analysis.

Flow cytometry for phenotypic analysis. Surface staining with fluorochrome-conjugated antibodies was performed in PBS together with live/dead staining (LIVE/DEAD® Fixable Violet Dead Cell Stain Kit, ViVid, Invitrogen) for 20 min at room temperature. Intracellular staining for CD68 and FOXP3 was performed according to manufacturer's instructions (eBioscience). Staining was measured with a CyAn ADP 9 flow cytometer (Beckman Coulter) and data were analyzed with FlowJo

software (TreeStar). All antibodies used in this study (listed in *Supplemental Materials and Methods*) were purchased from BioLegend, BD Biosciences, Beckman Coulter or eBioscience.

FACS sorting of T cells and TAMs from TILs and PBMCs. TILs and PBMCs were stained in sorting buffer (SB: PBS supplemented with 2% pooled human serum (PAA Laboratories) and 6 U/mL DNase I TypeIV (Sigma)) and stained with a mixture of fluorochrome-conjugated antibodies plus live-dead staining (LIVE/DEAD® Fixable Violet Dead Cell Stain Kit). After staining for 20 min at 4°C cells were washed and resuspended in SB. Gates were either placed on CD45$^+$CD8$^+$ T cells or on CD45$^+$CD4$^+$ T cells, or—in the case of the simultaneous sorting of T cells and myeloid cells—as shown in the gating strategy
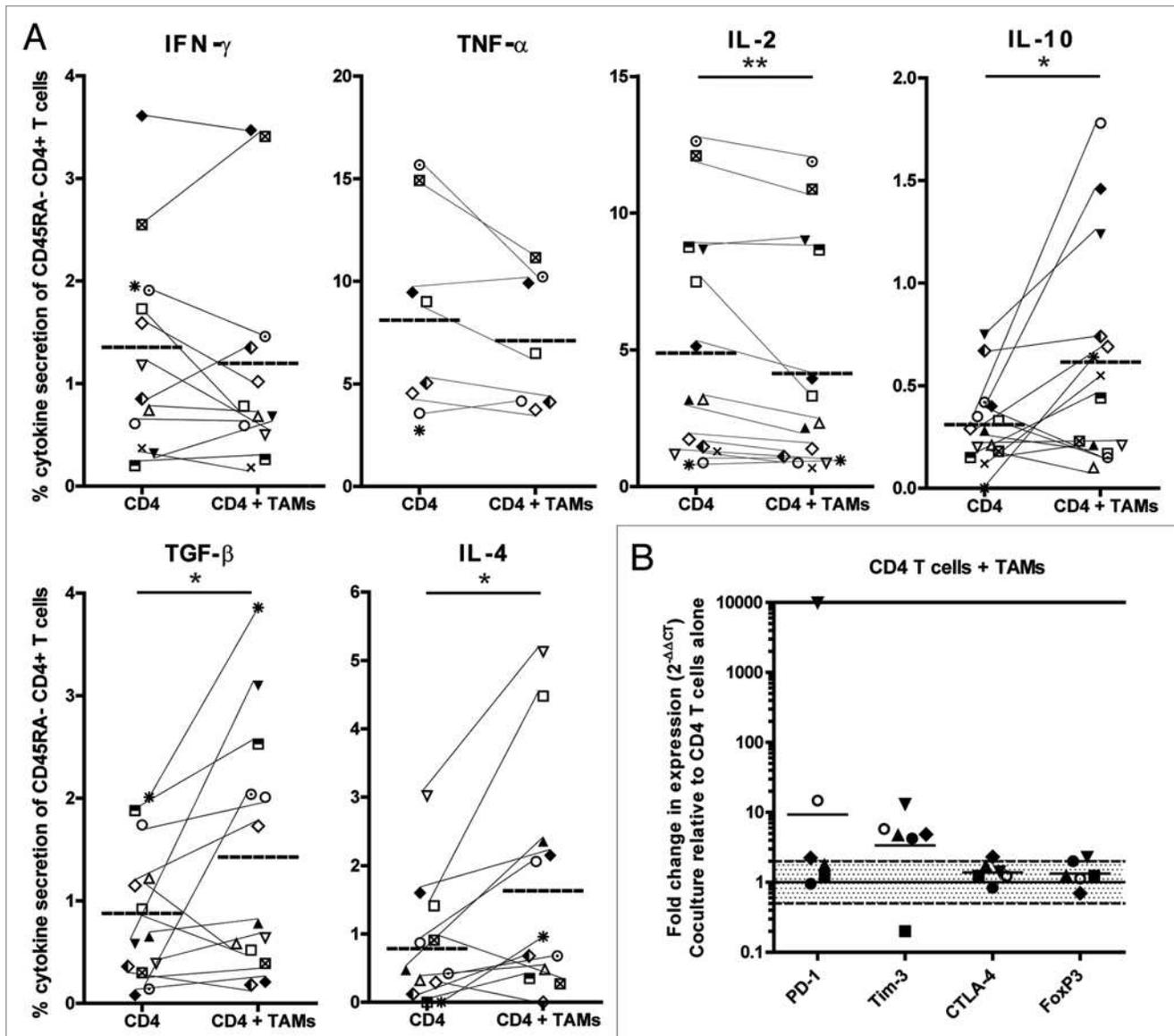
Figure 7. Clear cell renal cell carcinoma-derived M2 tumor-associated macrophages skew T cells toward a more regulated phenotype. (**A and B**) Sorted peripheral blood-derived CD4$^+$ T cells were cultured for 48 h with or without sorted autologous T$_2$ cells (CD45$^+$CD2$^-$CD19$^-$CD11b$^+$CD163^{high}) in a ratio of 1:1. (**A**) The production of cytokines was assessed via intracellular cytokine stating 6 h after ex vivo stimulation with anti-CD3/CD28 beads in the presence of brefeldin A and monensin upon gating on live CD45$^+$CD11b$^-$CD4$^+$ cells. Results of the same patient are connected by a thin line. The mean of each group and significant differences (* p < 0.05; ** p < 0.005) are depicted. (**B**) The expression of regulatory molecules was assessed by qRT-PCR. ΔCt levels were calculated by normalizing the Ct values of the target genes to the Ct values of *CD4*. Results are presented as fold change in expression level of CD4$^+$ T cells co-cultured in the presence of autologous T$_2$ (CD45$^+$CD2$^-$CD19$^-$CD11b$^+$CD163^{high}) cells relative to CD4$^+$ T cells cultured in their absence. Fold differences in expression within the shaded area are considered as not significant. The symbol at the 10,000 line on the y-axis represents a sample of which fold change could not be calculated, since expression was only detected after co-culture. Each symbol represents an individual patient.

(**Fig. S10**), and the different populations were sorted using a FACSAria III cell sorter (BD Biosciences).

Polyclonal stimulation and intracellular cytokine staining (ICS). After sorting, cells were allowed to rest overnight in a 96-well round-bottom plate in TC-RPMI (RPMI) (Gibco), supplemented with 2 g/L NaHCO$_3$ (Sigma), 2 mM L-glutamine (Sigma), 50 U/mL penicillin and 50 U/mL streptomycin (Gibco), 1× MEM nonessential amino acids (Gibco), 1 mM sodium pyruvate (Gibco), 100 μM β-mercaptoethanol (Sigma) and 10% pooled human serum plus 6 U/mL DNase I Type IV (Sigma)

T cells (at least 10,000 per well) were either cultured alone or with the tumor single-cell suspension or with TAMs (ratio 1:1). After the overnight resting period, T cells were stimulated in 96-well plates in the presence or absence of the tumor digest or TAMs with anti-CD3/CD28 Dynabeads (Invitrogen, 111.41D) (Ratio T cells:beads = 1:3) or with 50 ng/mL PMA (Sigma) plus 500 ng/mL ionomycin (Sigma). Stimulation was performed for 6 h at 37°C in TC-RPMI supplemented with 10 μg/mL brefeldin A (Sigma) and 6 U/mL DNase I Type IV (Sigma). Cells were surface-stained with a fluorochrome-conjugated

antibody cocktail including live-dead staining (LIVE/DEAD® Fixable Violet Dead Cell Stain Kit) in PBS for 20 min at room temperature in the dark. Subsequently, cells were fixed in 4% formalin (Kantonsapotheke Zürich) and permeabilized with permeabilization buffer (PB: PBS supplemented with 2% FCS, 20 mM EDTA, 0.05% NaN_3 and 0.1% saponin). For intracellular staining, cells were incubated with a mix of fluorescent-conjugated antibodies in PB for 20 min at room temperature in the dark. Cells were washed once with PB and resuspended in PBS containing 1% formalin before analysis by flow cytometry, as described above. The antibodies employed in this study are listed in *Supplemental Materials and Methods.* When the stimulation of T cells was performed in presence or absence of the tumor microenvironment, cytokine production was measured upon gating on ViViD⁻CD45⁺CD14⁻CD16⁻CD19⁻CD8⁺ or ViViD⁻CD45⁺CD14⁻CD16⁻CD19⁻CD4⁺ T cells, and—in presence or absence of TAMs—upon gating on ViViD⁻CD45⁺CD11b⁻CD4⁺ T cells.

RNA isolation. After FACS sorting or after co-culture experiments, a fraction of the cells (at least 500 cells) was resuspended in TRI Reagent (Ambion) and frozen at -80°C until RNA isolation. RNA was isolated using the MagMAX™-96 for Microarrays Total RNA isolation kit (AM1839 Ambion) by the No-Spin procedure, according to the manufacturer's instructions. RNA isolation from FFPE material was performed using Trizol, as described in *Supplemental Materials and Methods*.

Quantitative reverse transcription real-time PCR (qRT-PCR). The concentration and purity of RNA was evaluated using the NanoDrop ND-1000 spectrophotometer (NanoDrop Technologies). Five-hundred ng RNA were reverse transcribed using the high-capacity cDNA Reverse Transcription Kit (Applied Biosystems). Obtained cDNAs were stored at -20°C until qRT-PCR analysis. Because of limited material, cDNA of sorted cells and paraffin punches was pre-amplified. Pre-amplification was performed for 14 cycles according to manufacturer's instructions (TaqMan® PreAmp Master Mix Kit, Applied Biosystems). We tested the correlation of expression analyzed on original cDNA with that analyzed on pre-amplified cDNA for selected highly (CD45, CD68, CD163, TNFα, MHC-II) and lowly (iNOS, FOXP3, IL-10, IDO) expressed genes, and found an excellent correlation for all, confirming uniform pre-amplification for all samples (CD68 and CD163 are shown in **Fig. S3**). qRT-PCR was done on a Rotor-Gene Q real-time PCR cycler (Qiagen) using commercially available pre-developed TaqMan reagents with optimized primer and probe concentrations (TaqMan® gene expression assays, Applied Biosystems) (**Table S1**).

After an initial hold for 2 min at 50°C and 10 min at 95°C, probes were cycled 45 times at 95°C for 15 sec and at 60°C for 60 sec. All PCR reactions were performed in triplicates. Threshold cycle (Ct) values were determined with the Rotor-Gene Q Series software 1.7. ΔCt values were calculated by normalizing the target mRNA levels to (1) the endogenous control 18S rRNA (Hs03928990_g1), (2) the endogenous control *PPIA* mRNA (Hs99999904_m1) or (3) to the levels of *CD4* mRNA (Ct target gene-Ct control gene) as stated in the figure legends. Immune response-related transcripts other than *CD45* were normalized to the expression levels of *CD45*. Because there was no correlation between *CD45* transcripts and survival (**Fig. 1A**), this normalization will not obscure potential correlations between the expression of other immune response-related genes and survival. In some cases ΔCt levels were expressed as relative to the appropriate control. Therefore, ΔΔCt values were determined ((ΔCT target–ΔCT control)) and fold change calculated with the equation $2^{-\Delta\Delta Ct}$. Ct values > 38 were interpreted such that the gene was not expressed. Changes in the expression levels lower than 2-fold (both as upregulation and as downregulation) were considered as not significant. This range is illustrated as a shaded area in the figures.

Statistical analyses. The relationship between the expression of target genes and patient survival was analyzed using a univariate Cox proportional hazard regression model with 95% confidence intervals. The prognostic effect of variables that showed a correlation with survival in univariate analysis was tested for dependence on age at operation and tumor stage by multivariate Cox regression analysis. Furthermore, data was dichotomized based on mean gene expression value of all analyzed samples, log-rank test performed and Kaplan-Meier curves generated in which probability of overall survival was plotted over time. Correlations between different parameters were assessed using the Spearman Rho correlation test (IBM SPSS statistics software). Wilcoxon matched-pairs signed rank test was used to analyze statistical significance between groups (GraphPad Prism Software). The criterion for significance was set at $p \leq 0.05$.

Supplemental Material

Supplemental material may be downloaded here:
www.landesbioscience.com/journals/onco/article/23562/

References

1. Fridman WH, Pagès F, Sautès-Fridman C, Galon J. The immune contexture in human tumours: impact on clinical outcome. Nat Rev Cancer 2012; 12:298-306; PMID:22419253; http://dx.doi.org/10.1038/nrc3245.

2. Schreiber RD, Old LJ, Smyth MJ. Cancer immunoediting: integrating immunity's roles in cancer suppression and promotion. Science 2011; 331:1565-70; PMID:21436444; http://dx.doi.org/10.1126/science.1203486.

3. Beck C, Schreiber H, Rowley D. Role of TGF-beta in immune-evasion of cancer. Microsc Res Tech 2001; 52:387-95; PMID:11170297; http://dx.doi.org/10.1002/1097-0029(20010215)52:4<387::AID-JEMT1023>3.0.CO;2-W.

4. Kawamura K, Bahar R, Natsume W, Sakiyama S, Tagawa M. Secretion of interleukin-10 from murine colon carcinoma cells suppresses systemic antitumor immunity and impairs protective immunity induced against the tumors. Cancer Gene Ther 2002; 9:109-15; PMID:11916240; http://dx.doi.org/10.1038/sj.cgt.7700418.

5. Sica A, Schioppa T, Mantovani A, Allavena P. Tumour-associated macrophages are a distinct M2 polarised population promoting tumour progression: potential targets of anti-cancer therapy. Eur J Cancer 2006; 42:717-27; PMID:16520032; http://dx.doi.org/10.1016/j.ejca.2006.01.003.

6. Filipazzi P, Huber V, Rivoltini L. Phenotype, function and clinical implications of myeloid-derived suppressor cells in cancer patients. Cancer Immunol Immunother 2012; 61:255-63; PMID:22120756; http://dx.doi.org/10.1007/s00262-011-1161-9.

7. Facciabene A, Motz GT, Coukos G. T-regulatory cells: key players in tumor immune escape and angiogenesis. Cancer Res 2012; 72:2162-71; PMID:22549946; http://dx.doi.org/10.1158/0008-5472.CAN-11-3687.

8. Lewis CE, Pollard JW. Distinct role of macrophages in different tumor microenvironments. Cancer Res 2006; 66:605-12; PMID:16423985; http://dx.doi.org/10.1158/0008-5472.CAN-05-4005.

9. Sica A, Larghi P, Mancino A, Rubino L, Porta C, Totaro MG, et al. Macrophage polarization in tumour progression. Semin Cancer Biol 2008; 18:349-55; PMID:18467122; http://dx.doi.org/10.1016/j.semcancer.2008.03.004.

10. Bailey C, Negus R, Morris A, Ziprin P, Goldin R, Allavena P, et al. Chemokine expression is associated with the accumulation of tumour associated macrophages (TAMs) and progression in human colorectal cancer. Clin Exp Metastasis 2007; 24:121-30; PMID:17390111; http://dx.doi.org/10.1007/s10585-007-9060-3.

11. Krausgruber T, Saliba D, Ryzhakov G, Lanfrancotti A, Blazek K, Udalova IA. IRF5 is required for late-phase TNF secretion by human dendritic cells. Blood 2010; 115:4421-30; PMID:20237317; http://dx.doi.org/10.1182/blood-2010-01-263020.

12. Keller R, Geiges M, Keist R. L-arginine-dependent reactive nitrogen intermediates as mediators of tumor cell killing by activated macrophages. Cancer Res 1990; 50:1421-5; PMID:2302707.

13. Satoh T, Takeuchi O, Vandenbon A, Yasuda K, Tanaka Y, Kumagai Y, et al. The Jmjd3-Irf4 axis regulates M2 macrophage polarization and host responses against helminth infection. Nat Immunol 2010; 11:936-44; PMID:20729857; http://dx.doi.org/10.1038/ni.1920.

14. Lau SK, Chu PG, Weiss LM. CD163: a specific marker of macrophages in paraffin-embedded tissue samples. Am J Clin Pathol 2004; 122:794-801; PMID:15491976; http://dx.doi.org/10.1309/QHD6YFN81KQXUUH6.

15. Stein M, Keshav S, Harris N, Gordon S. Interleukin 4 potently enhances murine macrophage mannose receptor activity: a marker of alternative immunologic macrophage activation. J Exp Med 1992; 176:287-92; PMID:1613462; http://dx.doi.org/10.1084/jem.176.1.287.

16. Martinez FO, Gordon S, Locati M, Mantovani A. Transcriptional profiling of the human monocyte-to-macrophage differentiation and polarization: new molecules and patterns of gene expression. J Immunol 2006; 177:7303-11; PMID:17082649.

17. Kutikov A, Egleston BL, Wong YN, Uzzo RG. Evaluating overall survival and competing risks of death in patients with localized renal cell carcinoma using a comprehensive nomogram. J Clin Oncol 2010; 28:311-7; PMID:19933918; http://dx.doi.org/10.1200/JCO.2009.22.4816.

18. Vickers MM, Heng DY. Prognostic and predictive biomarkers in renal cell carcinoma. Target Oncol 2010; 5:85-94; PMID:20582732; http://dx.doi.org/10.1007/s11523-010-0143-8.

19. Motzer RJ, Bander NH, Nanus DM. Renal-cell carcinoma. N Engl J Med 1996; 335:865-75; PMID:8778606; http://dx.doi.org/10.1056/NEJM199609193351207.

20. Gouttefangeas C, Stenzl A, Stevanovi S, Rammensee HG. Immunotherapy of renal cell carcinoma. Cancer Immunol Immunother 2007; 56:117-28; PMID:16676181; http://dx.doi.org/10.1007/s00262-006-0172-4.

21. Morra L, Rechsteiner M, Casagrande S, Duc Luu V, Santimaria R, Diener PA, et al. Relevance of periostin splice variants in renal cell carcinoma. Am J Pathol 2011; 179:1513-21; PMID:21763681; http://dx.doi.org/10.1016/j.ajpath.2011.05.035.

22. Pello OM, De Pizzol M, Mirolo M, Soucek L, Zammataro L, Amabile A, et al. Role of c-MYC in alternative activation of human macrophages and tumor-associated macrophage biology. Blood 2012; 119:411-21; PMID:22067385; http://dx.doi.org/10.1182/blood-2011-02-339911.

23. Mulders PF, Brouwers AH, Hulsbergen-van der Kaa CA, van Lin EN, Osanto S, de Mulder PH. Guideline 'Renal cell carcinoma'. Ned Tijdschr Geneeskd 2008; 152:376-80; PMID:18380384.

24. Qian BZ, Pollard JW. Macrophage diversity enhances tumor progression and metastasis. Cell 2010; 141:39-51; PMID:20371344; http://dx.doi.org/10.1016/j.cell.2010.03.014.

25. Patsialou A, Wyckoff J, Wang Y, Goswami S, Stanley ER, Condeelis JS. Invasion of human breast cancer cells in vivo requires both paracrine and autocrine loops involving the colony-stimulating factor-1 receptor. Cancer Res 2009; 69:9498-506; PMID:19934330; http://dx.doi.org/10.1158/0008-5472.CAN-09-1868.

26. Gertler F, Condeelis J. Metastasis: tumor cells becoming MENAcing. Trends Cell Biol 2011; 21:81-90; PMID:21071226; http://dx.doi.org/10.1016/j.tcb.2010.10.001.

27. Sallusto F, Geginat J, Lanzavecchia A. Central memory and effector memory T cell subsets: function, generation, and maintenance. Annu Rev Immunol 2004; 22:745-63; PMID:15032595; http://dx.doi.org/10.1146/annurev.immunol.22.012703.104702.

28. Wherry EJ, Ha SJ, Kaech SM, Haining WN, Sarkar S, Kalia V, et al. Molecular signature of CD8+ T cell exhaustion during chronic viral infection. Immunity 2007; 27:670-84; PMID:17950003; http://dx.doi.org/10.1016/j.immuni.2007.09.006.

29. Attig S, Hennenlotter J, Pawelec G, Klein G, Koch SD, Pircher H, et al. Simultaneous infiltration of polyfunctional effector and suppressor T cells into renal cell carcinomas. Cancer Res 2009; 69:8412-9; PMID:19843860; http://dx.doi.org/10.1158/0008-5472.CAN-09-0852.

30. Kuang DM, Zhao Q, Peng C, Xu J, Zhang JP, Wu C, et al. Activated monocytes in peritumoral stroma of hepatocellular carcinoma foster immune privilege and disease progression through PD-L1. J Exp Med 2009; 206:1327-37; PMID:19451266; http://dx.doi.org/10.1084/jem.20082173.

31. Savage ND, de Boer T, Walburg KV, Joosten SA, van Meijgaarden K, Geluk A, et al. Human anti-inflammatory macrophages induce Foxp3+ GITR+ CD25+ regulatory T cells, which suppress via membrane-bound TGFbeta-1. J Immunol 2008; 181:2220-6; PMID:18641362.

32. Vasievich EA, Huang L. The suppressive tumor microenvironment: a challenge in cancer immunotherapy. Mol Pharm 2011; 8:635-41; PMID:21545153; http://dx.doi.org/10.1021/mp1004228.

33. Nakano O, Sato M, Naito Y, Suzuki K, Orikasa S, Aizawa M, et al. Proliferative activity of intratumoral CD8(+) T-lymphocytes as a prognostic factor in human renal cell carcinoma: clinicopathologic demonstration of antitumor immunity. Cancer Res 2001; 61:5132-6; PMID:11431351.

34. Kondo T, Nakazawa H, Ito F, Hashimoto Y, Osaka Y, Futatsuyama K, et al. Favorable prognosis of renal cell carcinoma with increased expression of chemokines associated with a Th1-type immune response. Cancer Sci 2006; 97:780-6; PMID:16863511; http://dx.doi.org/10.1111/j.1349-7006.2006.00231.x.

35. Sakaguchi S. The origin of FOXP3-expressing CD4+ regulatory T cells: thymus or periphery. J Clin Invest 2003; 112:1310-2; PMID:14597756.

36. Griffiths RW, Elkord E, Gilham DE, Ramani V, Clarke N, Stern PL, et al. Frequency of regulatory T cells in renal cell carcinoma patients and investigation of correlation with survival. Cancer Immunol Immunother 2007; 56:1743-53; PMID:17487490; http://dx.doi.org/10.1007/s00262-007-0318-z.

37. Adotevi O, Pere H, Ravel P, Haicheur N, Badoual C, Merillon N, et al. A decrease of regulatory T cells correlates with overall survival after sunitinib-based anti-angiogenic therapy in metastatic renal cancer patients. J Immunother 2010; 33:991-8; PMID:20948437; http://dx.doi.org/10.1097/CJI.0b013e3181f4c208.

38. Hori S, Takahashi T, Sakaguchi S. Control of autoimmunity by naturally arising regulatory CD4+ T cells. Adv Immunol 2003; 81:331-71; PMID:14711059; http://dx.doi.org/10.1016/S0065-2776(03)81008-8.

39. Siddiqui SA, Frigola X, Bonne-Annee S, Mercader M, Kuntz SM, Krambeck AE, et al. Tumor-infiltrating Foxp3-CD4+CD25+ T cells predict poor survival in renal cell carcinoma. Clin Cancer Res 2007; 13:2075-81; PMID:17404089; http://dx.doi.org/10.1158/1078-0432.CCR-06-2139.

40. Li JF, Chu YW, Wang GM, Zhu TY, Rong RM, Hou J, et al. The prognostic value of peritumoral regulatory T cells and its correlation with intratumoral cyclooxygenase-2 expression in clear cell renal cell carcinoma. BJU Int 2009; 103:399-405; PMID:19021626; http://dx.doi.org/10.1111/j.1464-410X.2008.08151.x.

41. Holness CL, Simmons DL. Molecular cloning of CD68, a human macrophage marker related to lysosomal glycoproteins. Blood 1993; 81:1607-13; PMID:7680321.

42. Mills CD, Kincaid K, Alt JM, Heilman MJ, Hill AM. M-1/M-2 macrophages and the Th1/Th2 paradigm. J Immunol 2000; 164:6166-73; PMID:10843666.

43. Mantovani A, Sozzani S, Locati M, Allavena P, Sica A. Macrophage polarization: tumor-associated macrophages as a paradigm for polarized M2 mononuclear phagocytes. Trends Immunol 2002; 23:549-55; PMID:12401408; http://dx.doi.org/10.1016/S1471-4906(02)02302-5.

44. Gordon S, Martinez FO. Alternative activation of macrophages: mechanism and functions. Immunity 2010; 32:593-604; PMID:20510870; http://dx.doi.org/10.1016/j.immuni.2010.05.007.

45. Ropponen KM, Kellokoski JK, Lipponen PK, Eskelinen MJ, Alanne L, Alhava EM, et al. Expression of inducible nitric oxide synthase in colorectal cancer and its association with prognosis. Scand J Gastroenterol 2000; 35:1204-11; PMID:11145294; http://dx.doi.org/10.1080/003655200750056709.

46. Clear AJ, Lee AM, Calaminici M, Ramsay AG, Morris KJ, Hallam S, et al. Increased angiogenic sprouting in poor prognosis FL is associated with elevated numbers of CD163+ macrophages within the immediate sprouting microenvironment. Blood 2010; 115:5053-6; PMID:20375314; http://dx.doi.org/10.1182/blood-2009-11-253260.

47. Komohara Y, Ohnishi K, Kuratsu J, Takeya M. Possible involvement of the M2 anti-inflammatory macrophage phenotype in growth of human gliomas. J Pathol 2008; 216:15-24; PMID:18553315; http://dx.doi.org/10.1002/path.2370.

48. Gabrilovich DI, Ostrand-Rosenberg S, Bronte V. Coordinated regulation of myeloid cells by tumours. Nat Rev Immunol 2012; 12:253-68; PMID:22437938; http://dx.doi.org/10.1038/nri3175.

49. Komohara Y, Hasita H, Ohnishi K, Fujiwara Y, Suzu S, Eto M, et al. Macrophage infiltration and its prognostic relevance in clear cell renal cell carcinoma. Cancer Sci 2011; 102:1424-31; PMID:21453387; http://dx.doi.org/10.1111/j.1349-7006.2011.01945.x.

50. Sato T, Terai M, Tamura Y, Alexeev V, Mastrangelo MJ, Selvan SR. Interleukin 10 in the tumor microenvironment: a target for anticancer immunotherapy. Immunol Res 2011; 51:170-82; PMID:22139852; http://dx.doi.org/10.1007/s12026-011-8262-6.

51. Daurkin I, Eruslanov E, Stoffs T, Perrin GQ, Algood C, Gilbert SM, et al. Tumor-associated macrophages mediate immunosuppression in the renal cancer microenvironment by activating the 15-lipoxygenase-2 pathway. Cancer Res 2011; 71:6400-9; PMID:21900394; http://dx.doi.org/10.1158/0008-5472.CAN-11-1261.

52. Fourcade J, Sun Z, Benallaoua M, Guillaume P, Luescher IF, Sander C, et al. Upregulation of Tim-3 and PD-1 expression is associated with tumor antigen-specific CD8+ T cell dysfunction in melanoma patients. J Exp Med 2010; 207:2175-86; PMID:20819923; http://dx.doi.org/10.1084/jem.20100637.